Article

Evolution of Structure and Properties of SBS-Modified Asphalt during Aging Process

Zhilong Cao [1], Qianlong Hao [1], Xin Qu [2,3,*], Kexin Qiu [1], Ruiqi Zhao [1] and Qianyu Liu [1]

[1] Department of Road and Railway Engineering, Beijing University of Technology, Beijing 100124, China; zhilongcao@bjut.edu.cn (Z.C.); haoqianlong@emails.bjut.edu.cn (Q.H.); olivia10qkx@163.com (K.Q.); zhaoruiqi@emails.bjut.edu.cn (R.Z.); liuqianyu@emails.bjut.edu.cn (Q.L.)
[2] School of Highway, Chang'an University, Xi'an 710064, China
[3] Key Laboratory of Intelligent Construction and Maintenance of CAAC, Xi'an 710064, China
* Correspondence: quxin@chd.edu.cn

Abstract: To explore the performance evolution mechanism of SBS-modified bitumen (SMB) during construction and service, the chemical structure, molecular weight and properties of styrene–butadiene–styrene triblock copolymer (SBS) and SMB under multiple aging levels were assessed via Fourier transform infrared spectroscopy (FTIR), gel permeation chromatography (GPC) and a dynamic shear rheometer (DSR). The results indicate that the polybutadiene segments in SBS are susceptible to oxidative degradation, and the molecular weight of SBS decreases rapidly during the aging process. The complex modulus and temperature sensitivity of SMB show relatively small changes during the early aging stage, which is mainly attributed to the impact of SBS oxidative degradation. While its temperature sensitivity decreases sharply after double PAV aging, it means the influence of asphalt aging on its performance is dominant. And there is a significant difference in the effect of aging on the creep recovery behavior of SMB under high and low shear stresses. The percentage recovery (R) of SMB decreases and then increases under low shear stress as aging progresses. While the value R of SMB increases gradually under high shear stress with the extension of aging. Meanwhile, the viscoelastic properties of SMB have gradually transformed to those of aged matrix asphalt after serious aging, which is also confirmed by the gradual destruction and degradation of the SBS cross-linked network in the binder from a fluorescence micrograph. This research will help to understand the performance failure mechanism of SMB during service, providing a theoretical reference for the selection of maintenance and renovation opportunities during the service process of SBS-modified asphalt pavement, as well as the avenue to achieve high-performance recycling.

Keywords: SBS-modified bitumen; aging behavior; molecular weight; creep and recovery rate; entropy elasticity; stiffness elasticity

1. Introduction

The viscoelastic properties of asphalt are of paramount merit for its wide application in pavement construction. In order to further improve the viscoelastic properties of asphalt to enhance the driving comfort and road capacity of asphalt pavement, polymer modifiers are widely used to modify asphalt [1], which include styrene–butadiene–styrene copolymer [2], crumb rubber [3], ethylene–vinylacetate copolymer [4], polyethylene [5], etc.

Polymer modifiers have good improvement effects on the high- and low-temperature properties and viscoelastic properties of asphalt. Ethylene–vinylacetate copolymer (EVA) can enhance the high-temperature performance of bitumen and lower its non-recoverable creep compliance [6], while EVA cannot form a networked structure in the bitumen [7], and EVA-modified bitumen is highly susceptible to strain at intermediate temperatures [8]. Mashaan et al. [9] reported that waste polyethylene terephthalate (PET) plastic can significantly improve the rutting and aging resistance of asphalt binder, and the ideal content

of waste plastic is 6–8%. Polyphosphate (PPA) could increase the m-value of bitumen and make it less susceptible to non-load-related cracking [10], and it was found [11,12] that PPA can promote the high-temperature deformation resistance and elastic recovery ability of bitumen. Crumb rubber (CR) can improve the high- and low-temperature performance of asphalt, and asphalt showed stiffer and greater elasticity after being modified using CR [13]. Duan et al. [14] modified asphalt using CR treated by microwaves and CR rich in deodorants and found that both of which can improve the high-temperature performance of asphalt, and the latter had a greater positive impact on its elastic recovery and deformation resistance. However, the most recommended polymer modifier is SBS. Zhang et al. [15] found SBS could boost the low-temperature creep performance of asphalt, but its aging resistance also had a large increase after modification. The rutting resistance and fatigue performance of asphalt modified with SBS also showed a significant improvement [16]. Babagoli et al. [17] reported that a 3% SBS modifier could significantly improve the percentage recovery and internal stress sensitivity of asphalt. Some researchers have found that there is a strong linear relationship between the percentage recovery of SBS-modified bitumen (SMB) and its non-recoverable creep compliance; this relationship is not related to the stress level but rather to the test temperature [18], although this point is controversial. And sulfur can increase the crosslinking density of SBS in SMB, further enhancing its elasticity, especially its ability to delay elastic recovery.

Obviously, SBS can improve the viscoelasticity of asphalt and significantly enhance its service performance [19]. However, SMB is inevitably affected by aging during construction and service. And the aging would change the composition and structure of both the SBS modifier and asphalt in SMB, which would directly affect the viscoelastic properties of SMB and cause its performance failure [20]. Xu et al. [21] studied the effect of aging on the viscosity and tensile properties of SBS-modified asphalt through a viscosity test, a force ductility test and a molecular dynamics simulation. It was found that the interface adhesion energy of modified asphalt–silica increased with the aging of SBS and asphalt, SBS and asphalt jointly affected the performance of modified asphalt during the aging process, and the impact of SBS aging on the increase in viscosity and tensile yield stress was far less than that of asphalt aging. And Yu et al. [22] found that aging would lead to the transformation of colloidal structure and the deterioration of asphalt binder performance. Meanwhile, the network structure formed in SMB would also be destroyed, which results in a great change in its rheological properties. It means the structure change of asphalt and SBS will affect the service behavior and life of SMB pavement in service [23]. Therefore, it is also necessary to consider how to restore the role of aged SBS modifiers in modified asphalt for achieving comprehensive performance recovery of aged SMBs. Eltwati et al. [24] reported that the combination of fresh SBS and aromatic oil can comprehensively restore the overall performance of mixtures and binders with high RAP content. And Wang et al. [25] conducted more in-depth research. Wang et al. conducted direct aging and rejuvenation treatments on SBS modifiers and then prepared MAAC (asphalt modified with aged SBS) and MARC (asphalt modified with rejuvenated SBS). The testing results showed that the aged SBS would deteriorate the physical properties of SMB with a higher possibility of generating cracks at lower temperatures, while rejuvenated SBS could improve MAAC's viscoelasticity. Namely, the structure of the SBS modifier and its cross-linking network state in asphalt directly affect the performance of SMB. However, there is still a lack of systematic research on the structural evolution law of SBS and how it affects the performance of modified asphalt during the aging process. This work will investigate the evolution of the chemical structure and molecular weight of SBS, as well as the chemical structure and performance degradation laws of SMB during construction and service through indoor simulation aging, and analyze the correlation between them.

To investigate the aging behavior and performance evolution mechanism of SMB during the aging process, samples of SBS modifier and SMB with multiple aging levels were prepared. The chemical structure and molecular weight of SBS with different aging degrees were characterized using FTIR and GPC tests. Meanwhile, the chemical structure, molecular

weight, physical–rheological performances, creep-recovery properties and fluorescence micrograph of SMB with multiple aging levels were also characterized and analyzed. The research results are expected to contribute to an in-depth understanding of the performance failure mechanism of SMB during service, which could provide a theoretical reference for the selection of maintenance and renovation opportunities during the service process of SBS-modified asphalt pavement, as well as how to achieve high-performance recycling of waste SBS-modified asphalt mixture.

2. Materials and Methods

2.1. Materials

The properties of asphalt used in this research are listed in Table 1. SBS with a block ratio (PS/PB) of 30/70 is used as a modifier in this work. Asphalt and SBS modifiers were mixed using the melt blending method to prepare SBS-modified asphalt (SMB), and the properties of SMB are also listed in Table 1. Compared to the matrix asphalt, the penetration of SMB decreases, while the ductility, viscosity and softening point of SMB all have a significant increase. It means the high-temperature performance and low-temperature toughness of asphalt all have a significant improvement after the modification with SBS.

Table 1. The base properties of raw asphalt.

	Penetration 25 °C/0.1 mm	Ductility/cm	Softening Point/°C	Viscosity 135 °C/Pa·s
Asphalt	71	13.5 (10 °C)	49.5	0.49
SMB	51	32.5 (5 °C)	69.5	2.68

2.2. Aging Method for SBS Modifier and SBS-Modified Bitumen

SMB and SBS modifiers were subjected to TFOT aging and multiple PAV aging successively. The specific aging methods and sample labels are shown in Table 2. The scheme of the entire experiment is displayed in Figure 1.

Table 2. Specific aging method for SMB and SBS.

Sample	Aging Method	Sample	Aging Method
SMB	No aging	SBS	No aging
T-SMB	TFOT	T-SBS	TFOT
TP-SMB	TFOT + PAV	TP-SBS	TFOT + PAV
T2P-SMB	TFOT + 2PAV	T2P-SBS	TFOT + 2PAV
T3P-SMB	TFOT + 3PAV	T3P-SBS	TFOT + 3PAV
T4P-SMB	TFOT + 4PAV	T4P-SBS	TFOT + 4PAV

2.3. FTIR Test

The chemical structure of SMB and SBS modifiers was characterized using a Spectrum II Fourier transform infrared spectrometer in this work. This test was performed in ATR mode with a scanning frequency of 16 and a wavenumber range of 4000~500 cm^{-1} at a resolution of 4 cm^{-1}.

2.4. Mass Change Measurement

The mass change rate (MR) of SBS can be measured and calculated using Equation (1).

$$MR(\%) = \frac{M_a - M_0}{M_0} \times 100\%$$ (1)

where M_0 and M_a refer to the mass of samples before and after aging, respectively.
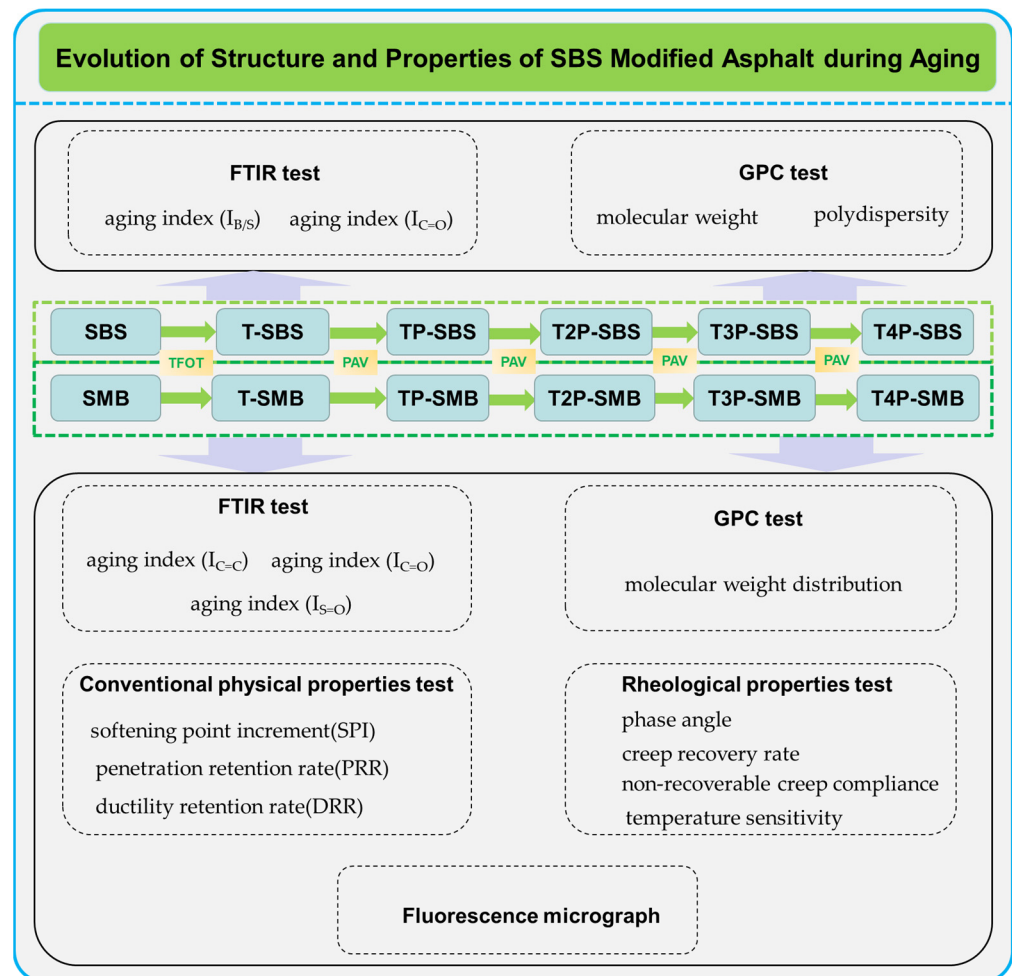
Figure 1. The scheme of the entire experiment.

2.5. GPC Test

The gel permeation chromatography test can be divided into the following steps: (1) Weigh samples and dissolve them into tetrahydrofuran in a bottle with a concentration of 2.5%. (2) Keep 3 days' standing of the solution to ensure that the asphalt and SBS modifier dissolve into tetrahydrofuran completely. (3) Inject 2 mL of the solution into the sample bottle through a 0.45 um filter to remove impurity particles. (4) Inject 0.5 mL of the filtered solution into the gel permeation chromatograph. (5) Finally, carry out this test at a temperature of 25 °C with a flow rate of 1.0 mL/min.

2.6. Conventional Physical Properties Test

Conventional physical properties of SMB before and after aging, including softening point, ductility (5 °C), penetration (25 °C) and Brookfield rotational viscosity (135 °C), were tested according to the ASTM standard [26–29]. Softening point increment (SPI), penetration retention rate (PRR) and ductility retention rate (DRR) were used to evaluate the aging degree of SMB, which were calculated using the following equation.

$$\text{SPI} = \text{softening point of SMB after aging} - \text{softening point of SMB before aging}$$

$$\text{PRR} = (\text{penetration of SMB after aging} - \text{penetration of SMB before aging})/\text{penetration of SMB before aging}$$

$$\text{DRR} = (\text{ductility of SMB after aging} - \text{ductility of SMB before aging})/\text{ductility of SMB before aging}$$

2.7. Rheological Properties Test

The rheological properties of all binders were also tested. More test parameters are listed in Table 3.

Table 3. Rheological testing parameters of binders.

Temperature/°C	Plates Gap/mm	Plates Diameter/mm	Scanning Frequency/rad/s	Heating Rate/°C/min
−10~30	2	8	10	2
30~80	1	25	10	2

2.8. Multi-Stress Creep and Recovery Property Test

This MSCR test includes 20 cycles at 0.1 kPa and 10 cycles at 3.2 kPa; each cycle includes the loading for 1 s and the rest for 9 s and was conducted under different temperatures from 46 °C to 70 °C. The strain versus time curve was recorded in each cycle, and its schematic diagram is displayed in Figure 2. The percentage recovery (R) [30] and non-recovered creep compliance (J) are calculated using Equations (2) and (3). ε represents the strain of the specimen, and τ refers to the loading stress.

$$R_\tau = \frac{1}{10}\sum_{i=1}^{10}\left[\frac{\varepsilon_{c,i} - \varepsilon_{r,i}}{\varepsilon_{c,i} - \varepsilon_{r,i-1}} \times 100\%\right] \tag{2}$$

$$J_{\tau\ (kPa^{-1})} = \frac{1}{10}\sum_{i=1}^{10}\left[\frac{\varepsilon_{r,i} - \varepsilon_{r,i-1}}{\tau_{(kPa)}}\right] \tag{3}$$
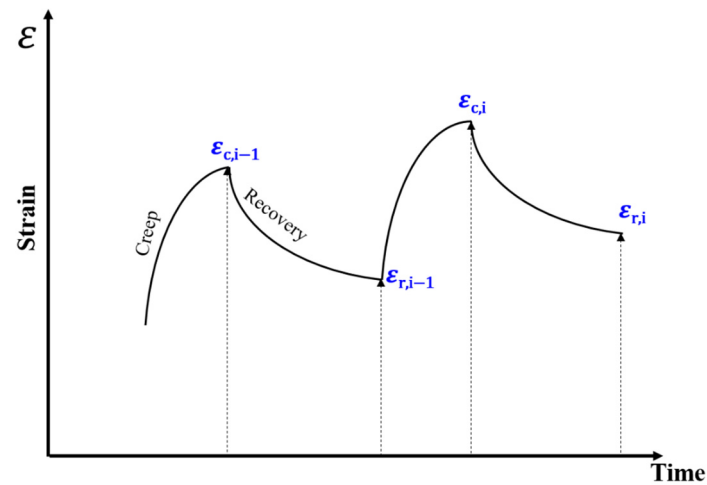

Figure 2. Schematic diagram of MSCR curves for binder.

3. Results and Discussions

3.1. Effect of Aging on Chemical Structure and Molecular Weight of SBS Modifier

3.1.1. Chemical Structure

The infrared spectra of different aged SBS modifiers are displayed in Figure 3. The peak at 699 cm^{-1} corresponds to the out-of-plane bending vibration of monosubstituted benzene in polystyrene (PS) segments. The peak at 969 cm^{-1} comes from the out-of-plane bending vibration of (trans)-CH= in polybutadiene (PB) segments. The intensity for 969 cm^{-1} decreases sharply after aging, while that for 699 cm^{-1} remains stable. It implies that the chemical stability of PS is much better than that of PB. Therefore, the aging index ($I_{B/S}$) [31] is recommended to evaluate the aging degree of SBS, whose computational formulas are listed in Equation (4).

$$I_{B/S} = \frac{A_{969}}{A_{699}} \tag{4}$$

$$I_{C=O} = \frac{A_{1720}}{A_{699}}$$ (5)

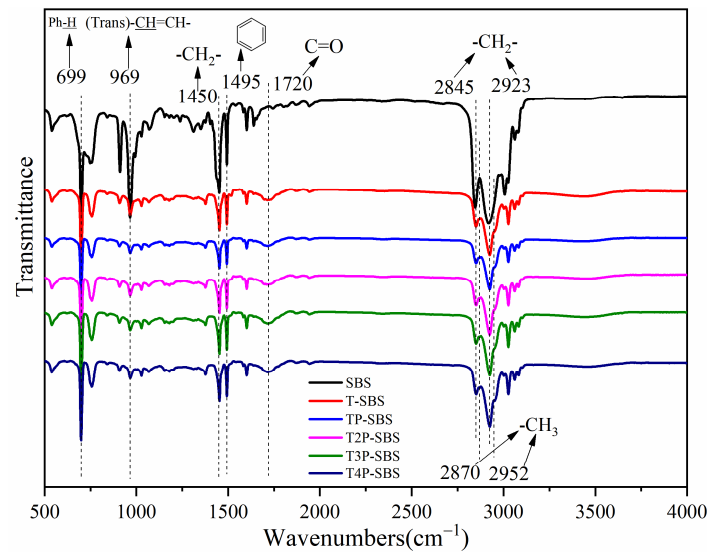where $A_{(XX)}$ refers the area of xx cm^{-1} peak.

Figure 3. FTIR spectra of different aged SBS.

Furthermore, the emerging absorption peak at 1720 cm^{-1} originates from the stretching vibration of the carbonyl group, and its intensity increases sharply with aging. It indicates that SBS is oxidized during aging. Another aging index ($I_{C=O}$) is calculated using Equation (5). The aging indexes of different aged SBS modifiers are shown in Figure 4. $I_{B/S}$ decreases from 1.68 to 0.17, and $I_{C=O}$ increases to 0.21 with the extension of aging, and their change rate in the early aging stage is far greater than that in the late aging stage. It means the PB segments in SBS have been severely damaged and oxidized during TFOT aging, implying that SBS is susceptible to aging alone in a high-temperature oxygen environment. The FTIR main characteristic peaks of aged SBS are listed in Table 4, and 2870 cm^{-1} and 2952 cm^{-1} belong to the symmetric and asymmetric stretching vibrations of methyl, respectively. 1450 cm^{-1} ascribes to the out-of-plane bending vibration of methylene, and 2845 cm^{-1} and 2923 cm^{-1} also originate from methylene; their intensity all has a decrease. These results suggest the PB segments in SBS gradually undergo oxidative degradation with aging.
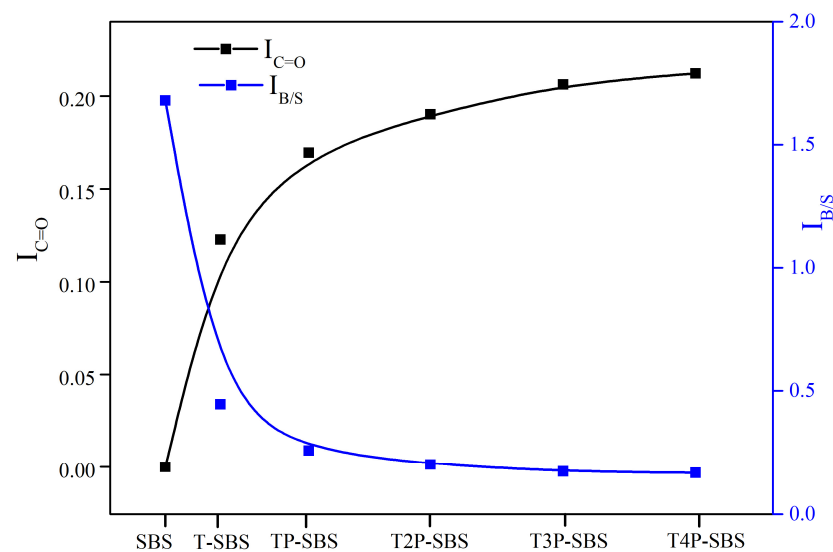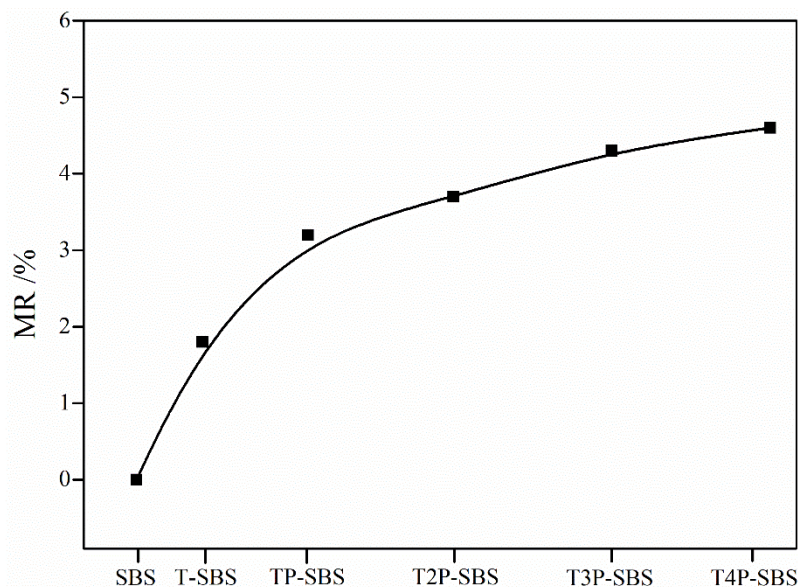

Figure 4. Aging indexes of different aged SBS modifiers.

Table 4. FTIR main characteristic peaks of aged SBS.

Wavenumber/cm^{-1}	Group	Structure	Vibration Type
699	styrene	Ph-H	Out-of-plane bending vibration of monosubstituted benzene
969	butadiene	(trans)-CH=CH	Out-of-plane bending vibration
1450	methylene	-CH$_2$-	Out-of-plane bending vibration
1495	benzene	⬡	Benzene ring skeleton vibration
1720	carbonyl	C=O	Stretching vibration
2845	methylene	-CH$_2$-	Symmetric stretching vibration
2870	methyl	-CH$_3$	Symmetric stretching vibration
2923	methylene	-CH$_2$-	Asymmetrical stretching vibration
2952	methyl	-CH$_3$	Asymmetrical stretching vibration

3.1.2. Mass Change

The mass change rate of different aged SBS modifiers is depicted in Figure 5. The value of MR is positive and gradually increases. It means SBS has undergone a violent oxidation reaction during the direct aging process, and the increasing oxygen content in SBS enhances its mass.

Figure 5. Mass change rate of different aged SBS modifiers.

3.1.3. Molecular Weight

The GPC curves of different aged SBS modifiers are illustrated in Figure 6. The GPC curves of SBS shift to the right after TFOT short-term aging, and they further shift slowly during PAV long-term aging. The average molecular weight decreases by 90.6% after direct thermal-oxygen aging at 163 °C for 5 h (Figure 7), and its polydispersity increases largely. In the subsequent PAV aging, the molecular weight of SBS decreases slowly, and its polydispersity also decreases gradually. These results indicate that high temperatures are more likely to lead to the degradation of SBS molecules, and SBS has been seriously degraded with significantly decreased molecular weight in the TFOT aging stage. Combined with Section 3.1.1, the results show that the oxidative degradation of SBS is mainly initiated by C=C bonds in PB segments. And the SBS aging reaction mechanism can be described as depicted in Figure 8 [32].
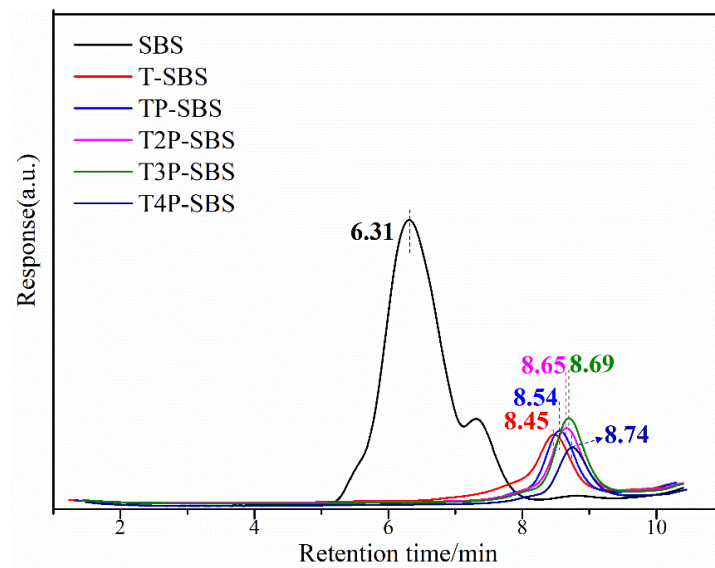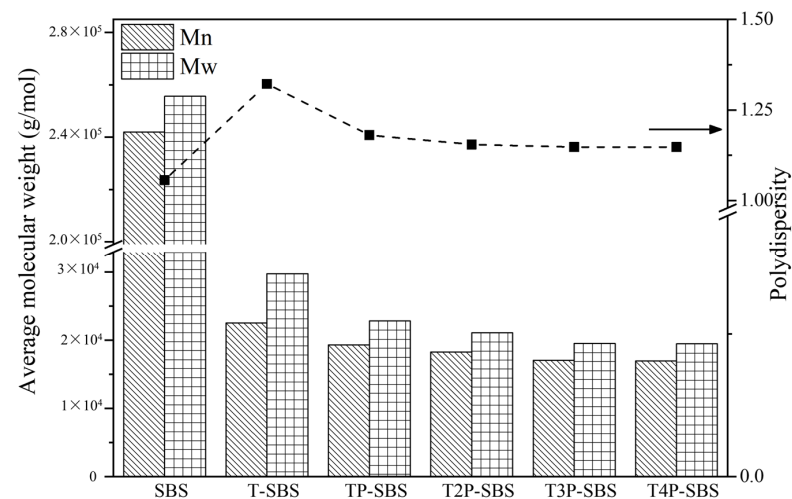
Figure 6. GPC curves of different aged SBS modifiers.

Figure 7. Average molecular weight and polydispersity of different aged SBS modifiers.
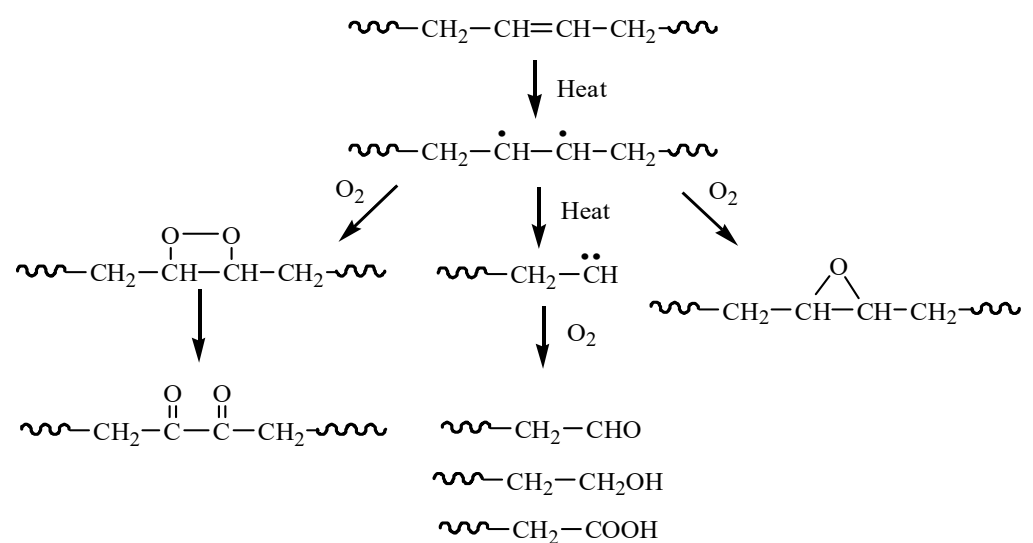

Figure 8. SBS aging reaction mechanism induced by C=C structures [25].

3.2. Effect of Aging on Chemical Structure and Properties of SBS-Modified Bitumen

3.2.1. Chemical Structure

The infrared spectra of different aged SMBs are displayed in Figure 9. Obviously, the absorption peak (1030 cm^{-1} and 1700 cm^{-1}) intensity of oxygen-containing groups gradually increases, and the intensity of characteristic absorption peaks for PB segments in the SBS modifier is gradually weakened. This indicates that SBS and asphalt in SMB are gradually oxidized. Three aging indexes are selected to analyze the aging degree of SMB, and their computational formulas are listed in Equations (6)–(8) [33].

$$I_{C=C} = \frac{A_{969}}{A_{700\sim3000}} \tag{6}$$

$$I_{S=O} = \frac{A_{1030}}{A_{700\sim3000}} \tag{7}$$

$$I_{C=O} = \frac{A_{1700}}{A_{700\sim3000}} \tag{8}$$

where $A_{(xx)}$ refers to the area of the xx cm^{-1} peak and $A_{(700\sim3000)}$ represents the sum of all absorption peak areas between 700 cm^{-1} and 3000 cm^{-1}.
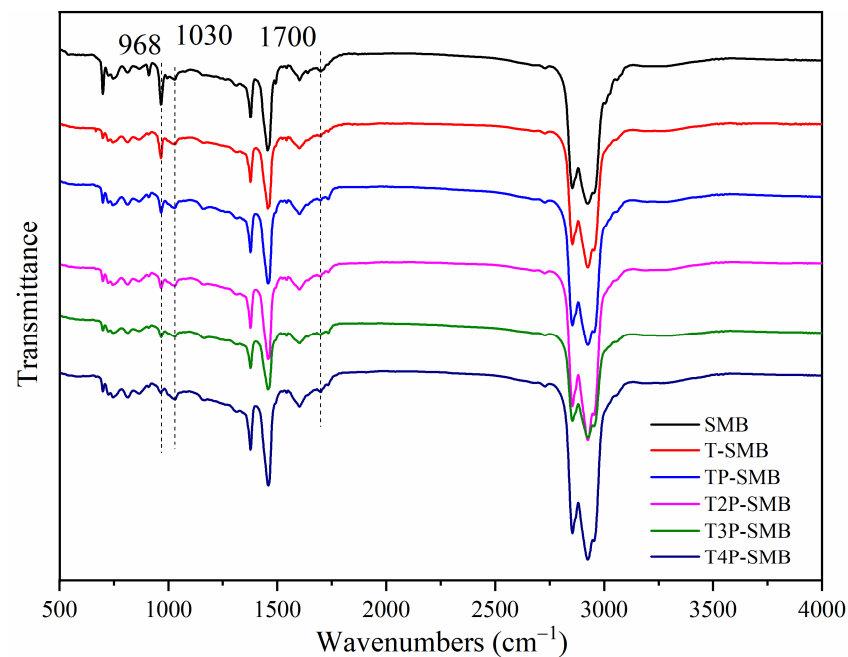

Figure 9. Infrared spectra of different aged SMBs.

The aging indexes of different aged SMBs are depicted in Figure 10. $I_{S=O}$ and $I_{C=O}$ increase with the extension of the aging process, and the growth rate of $I_{C=O}$ for SMB is much lower than that of SBS in Section 3.1.1, which indicates the aging resistance of the SBS polymer inside asphalt is better than that of the SBS modifier. Meanwhile, the declining rate of $I_{C=C}$ for SMB is also lower than that for SBS. The physical blocking effect of asphalt on oxygen slows down the oxygen permeation rate and reduces its contact concentration with SBS, thus delaying the aging process of SBS in a binder.
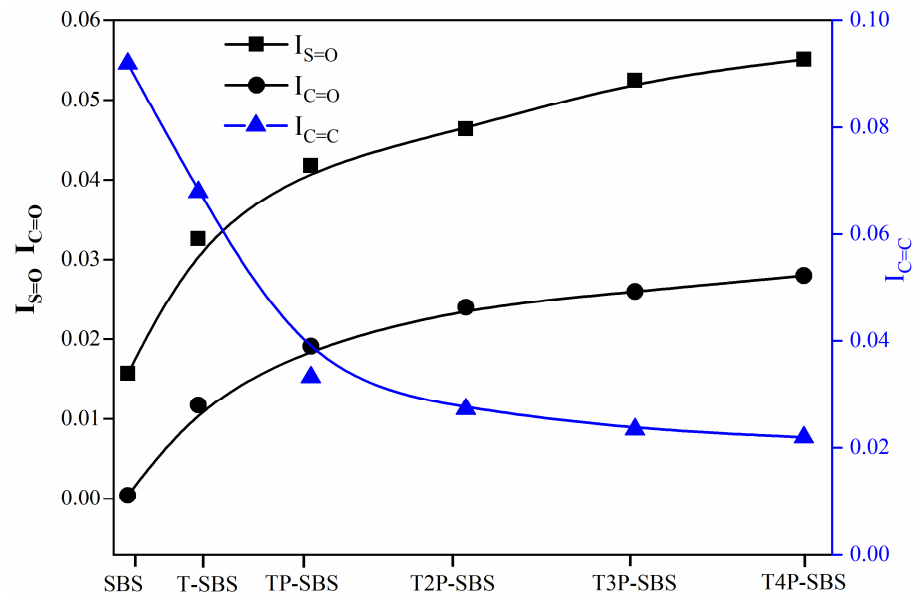
Figure 10. Aging indexes of different aged SMBs.

3.2.2. Molecular Weight

The molecular weight distribution of different aged SMBs is shown in Figure 11. The main leaching peak on the right side belongs to asphalt in SMB, while the small leaching peak on the left is attributed to SBS in SMB. It can be seen from the partially enlarged view that the leaching peak area for SBS decreases, and its position gradually shifts to the right. After careful observation, it can be found that the SBS leaching peak for T2P-SMB is very small, and that for T3P-SMB and T4P-SMB almost disappears. It suggests that the oxidative degradation of SBS in binders is not significant in the construction and early service stages. SBS in SMB has been seriously degraded after TFOT aging and double PAV aging, and further aging tests will lead to the complete degradation of SBS into small molecules, implying that SBS will be completely oxidized and degraded in the later service stage.
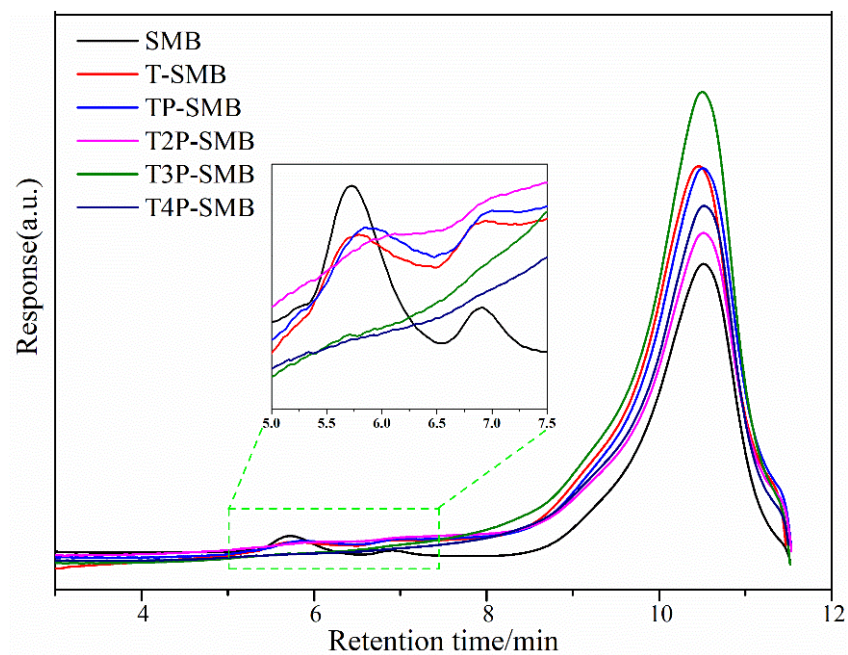

Figure 11. Molecular weight distribution of different aged SMBs.

The common rejuvenation method only focuses on the restoration of the colloidal structure of aged SMB. However, the SBS modifier and the construction of the SBS cross-linking network in the binder play an important role in improving the high- and low-temperature performance of the binder. Based on the aging mechanism of SMB, the reactive rejuvenator system includes common and reactive rejuvenators. The common rejuvenator is used to re-balance the asphalt component in aged SMB, and the reactive rejuvenator is utilized for reconstructing its crosslinking network structure in aged SMB. Therefore, the destroyed SBS crosslinking structure in a binder would be reconstructed using a structural repair agent, so the aged SMB with the aging level of T2P-SMB is recommended to be high-value recycled using the reactive rejuvenation method [34]. For the aged SMB with a more serious aging level than T2P-SMB, it is recommended to be recycled using a common rejuvenation method since its SBS crosslinking structure in the binder was completely degraded [35]. Namely, GPC curve analysis could also provide a new perspective on the selection of appropriate rejuvenation methods for aged SBS-modified asphalt.

3.2.3. Physical Properties

The physical aging indexes [36] (softening point increment (SPI), penetration retention rate (PRR) and ductility retention rate (DRR)) of different aged SMBs are displayed in Figure 12. The values of PRR and DRR decrease as aging progresses, and DRR decreases to 4.1% for T2P-SMB, which indicates that SMB gradually hardens and embrittles during aging, and the low-temperature ductility has seriously deteriorated after TFOT and double PAV aging. It is noteworthy that the value of SPI for T-SMB is -1.5 °C, which implies the high-temperature performance of SMB is slightly reduced. According to the analysis in the above section, SBS in SMB will undergo oxidative degradation during the aging process, which leads to a decreased softening point. Meanwhile, asphalt in SMB will undergo oxidative polycondensation, which will cause an increasing softening point. Obviously, the oxidation degradation of SBS dominates the high-temperature performance of SMB in the early aging stage, while the oxidation of asphalt dominates in the subsequent long-term aging process.
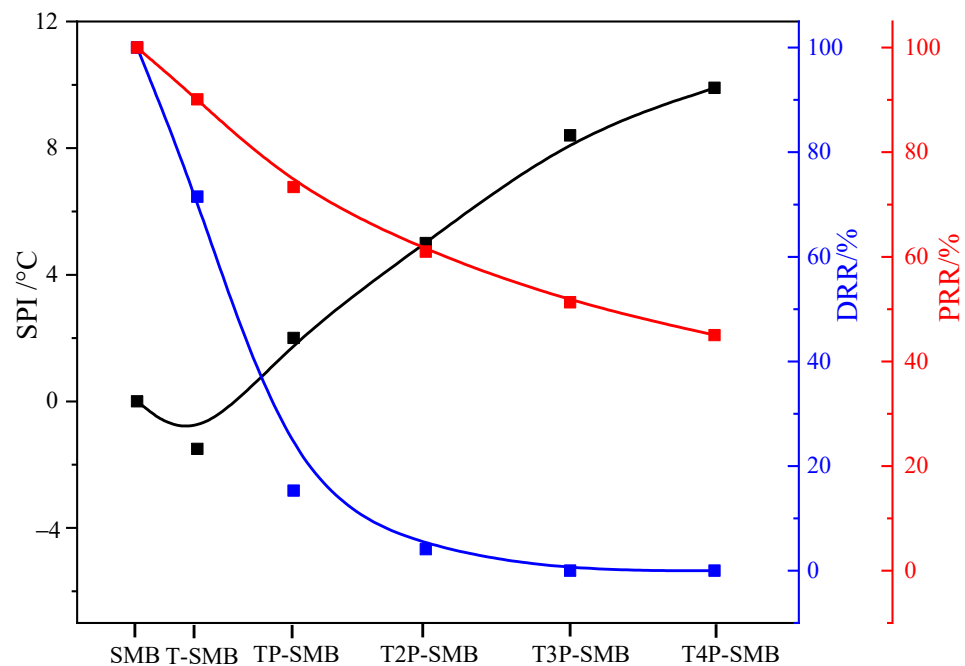

Figure 12. Physical properties change index of different aged SMBs.

3.2.4. Rheological Properties

G* and δ of different aged SMBs are displayed in Figure 13. From Figure 13a, the G* for SMB, T-SMB and TP-SMB changes slightly due to the combined action of SBS oxidative

degradation and asphalt oxidative hardening during aging. It suggests that the change in G* for SMB is not significant in the construction and early service stages. While the G* for T3P-SMB and T4P-SMB increases largely, this is because SBS has been completely degraded after TFOT and three times PAV aging from Section 3.2.2, and the oxidation hardening of asphalt has completely dominated the complex modulus growth of SMB. The entropy elasticity of the SBS cross-linked network structure can inhibit the transition of SMB from a highly elastic state to a viscous flow state within a certain temperature range, resulting in the formation of a phase angle plateau. Therefore, the appearance of the phase angle platform region indicates the formation of the SBS cross-linking network structure in SMB. The narrowing of the platform area means that the ability of SBS modifiers to inhibit the state transition of SMB is weakened, which suggests the damaged SBS cross-linking network structure and the degraded molecular structure. From Figure 13b, the phase angle platform of SMB shifts towards high temperature after TFOT aging, and that of TP-SMB disappears, which means the SBS cross-linked network in SMB has been broken after TFOT and PAV aging. The δ for TP-SMB is greatly reduced as the aging continues owing to the oxidation-hardening of asphalt. It implies that the stiffness, elasticity and deformation resistance of SMB will be greatly enhanced in the later service stage.
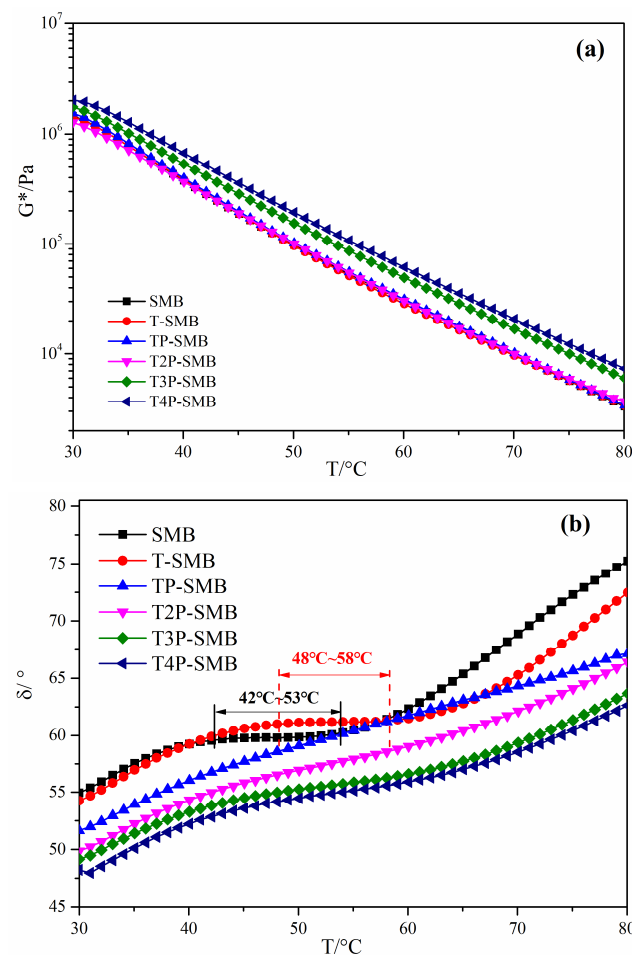

Figure 13. Complex modulus and phase angle of different aged SMBs (**a**): complex modulus; (**b**): phase angle.

Temperature sensitivity could be another index to analyze the aging behavior of SMBs; the temperature sensitivity of different aged SMBs is shown in Figure 14. The fitting analysis results of the relationship between logG* and T are listed in Table 5. The absolute value ($|K|$) of slope can be used to evaluate the temperature sensitivity of the binder, and a higher value of $|K|$ means better temperature sensitivity. The analysis results are shown

in Figure 14b. The temperature sensitivity of SMB is basically unchanged after TFOT and PAV aging, while its temperature sensitivity is greatly reduced as it continues to age. The destroyed SBS cross-linking structure in SMB and the small molecules produced by the oxidative degradation of SBS during the aging process will benefit from enhancing the temperature sensitivity of SMB. However, the aging of asphalt will increase the content of heavy components (including resin and asphaltene) in SMB, which will lead to a reduction in its temperature sensitivity. Obviously, the complex modulus–the temperature sensitivity of aged SMB is influenced by these two aspects. It suggests that the change in temperature sensitivity for SMB is not significant in the construction and early service stages. However, as the aging continues, the asphalt continues to be deeply aged, and its influence on the temperature sensitivity of SMB is dominant. After T3P aging, the temperature sensitivity of SMB seems to be stable again after the previous decrease, which is attributed to the combined effect of SBS oxidation degradation and asphalt oxidation hardening.
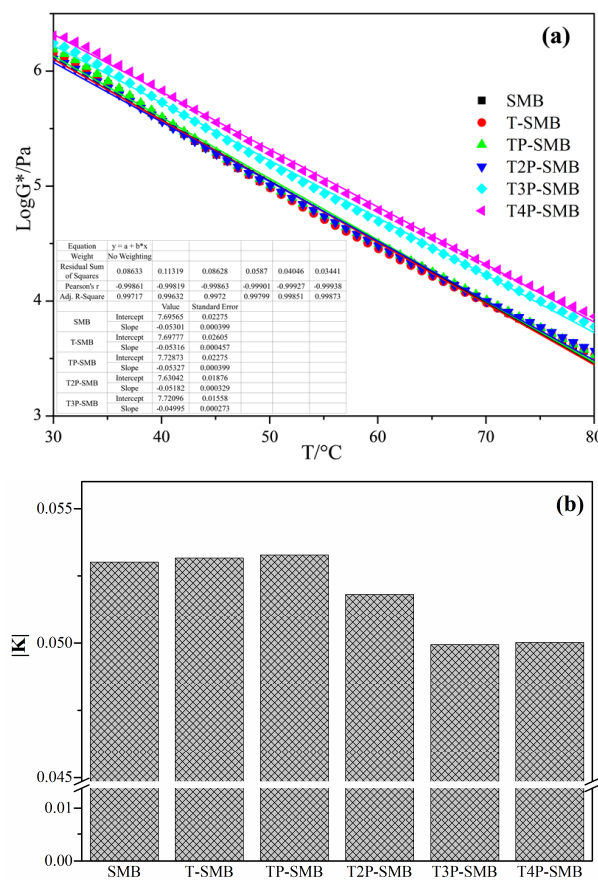

Figure 14. Temperature sensitivity of different aged SMBs (**a**): relationship between complex modulus and temperature; (**b**): temperature sensitivity.

Table 5. Complex modulus–temperature sensitivity equation of all binders.

Sample	LogG* = KT + B
SMB	LogG* = −0.05301T + 7.69565
T-SMB	LogG* = −0.05316T + 7.69777
TP-SMB	LogG* = −0.05327T + 7.72873
T2P-SMB	LogG* = −0.05182T + 7.63042
T3P-SMB	LogG* = −0.04995T + 7.72096
T4P-SMB	LogG* = −0.05003T + 7.82036

3.2.5. Multi-Stress Creep and Recovery Property

Percentage Recovery and Non-Recoverable Creep Compliance

The percentage recovery of aged SMBs is shown in Figure 15. The $R_{3.2}$ value of SMB first increases with the deepening of the aging degree, then tends to be flat, and then increases significantly from Figure 15a. Explicitly, aging has a more significant influence on $R_{3.2}$ of SMB at higher temperatures. Figure 15b shows that the $R_{0.1}$ value of SMB first decreases and then increases under low shear stress with the extension of aging time. The creep recovery ability of SMB is mainly attributed to the entropy elasticity of the SBS cross-linked structure and the stiffness elasticity of asphalt. Figure 16a shows that aging is beneficial for reducing the value $J_{3.2}$ of SMB, and it is most evident at high temperatures of 64 °C and 70 °C, while $J_{0.1}$ of SMB increases and then decreases with the extension of aging time. The value $J_{0.1}$ for SMB to TP-SMB rises gradually, while their $R_{0.1}$ shows a decreasing trend. This is because the destruction of the SBS cross-linked network leads to a decrease in the entropy elasticity of SMB, while the stiffness elasticity of asphalt in the binder is insufficient. The percentage recovery $R_{0.1}$ for T2P-SMB to T4P-SMB rises gradually, which is attributed to the increase in stiffness elasticity from aged asphalt in binder. The stiffness elasticity of asphalt is caused by the change in intramolecular energy, which is similar to the elastic recovery ability of spring. There is an obvious correlation between the stiffness elasticity of asphalt and its mechanical properties [37], which is also confirmed by the raising complex modulus for T2P-SMB to T4P-SMB from Section 3.2.4. It also suggests that the viscoelastic properties of SMB change from polymer-modified asphalt to matrix asphalt after serious aging.
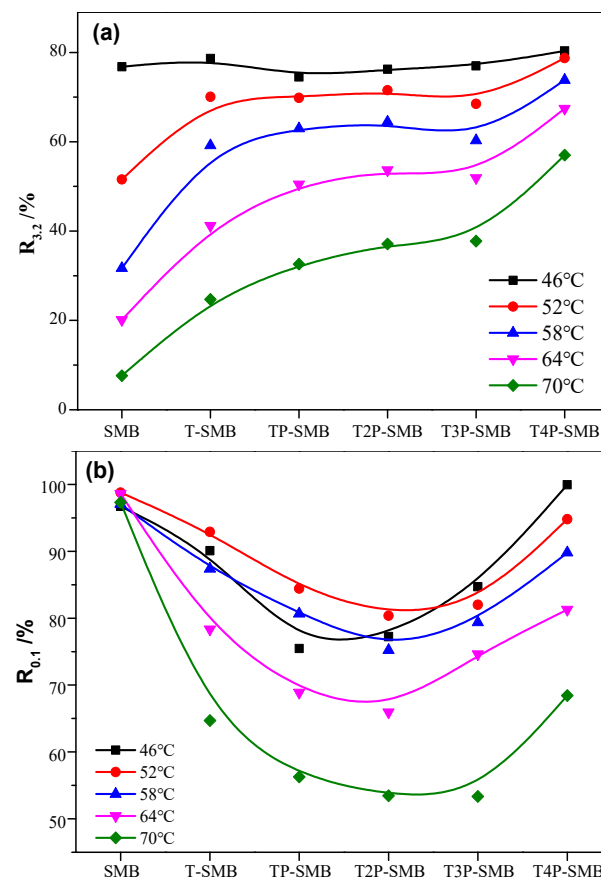

Figure 15. Percentage recovery of different aged SMBs (**a**): percentage recovery under 3.2 kPa; (**b**): percentage recovery under 0.1 kPa.
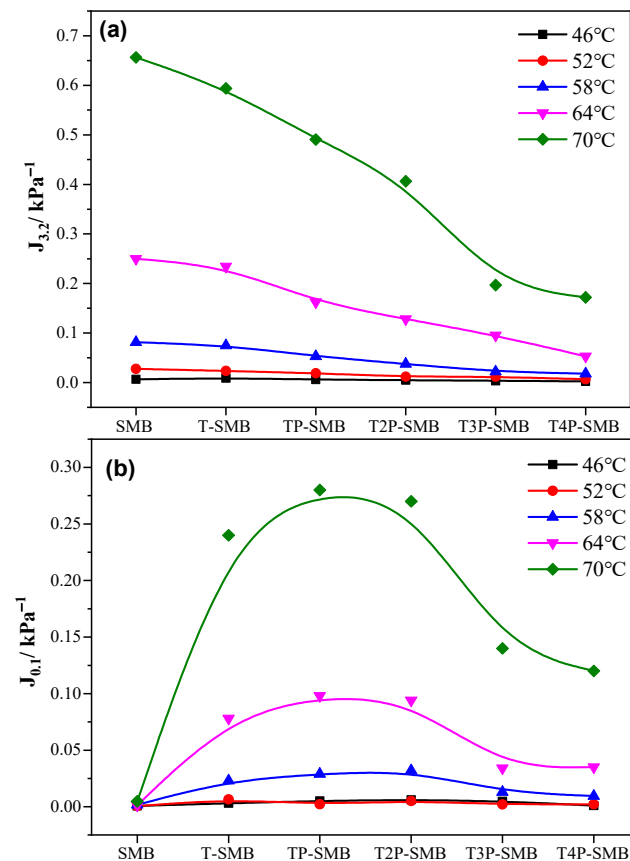
Figure 16. Non-recoverable creep compliance of different aged SMBs (**a**): non-recoverable creep compliance under 3.2 kPa; (**b**): non-recoverable creep compliance under 0.1 kPa.

Percentage Recovery Temperature Sensitivity

The percentage recovery temperature sensitivity curves of different aged SMBs and their analysis results are shown in Figure 17 and Table 6, respectively. Obviously, there is a significant temperature-sensitivity difference in the creep recovery ability of SMB with different aging degrees under high and low shear stress. The percentage recovery temperature sensitivity coefficient ($|K|$) of SMB decreases gradually with the increase in aging degree under high shear stress (3.2 kPa). The percentage recovery temperature sensitivity coefficient ($|K|$) of SMB shows a trend of increasing first, then decreasing, and then increasing with the deepening of aging under low shear stress (0.1 kPa). The entropy elasticity of SBS is less sensitive to temperature; the oxidative degradation of SBS in SMB during aging would enhance the temperature sensitivity. The temperature sensitivity of $R_{0.1}$ is much lower than that of $R_{3.2}$ for SMB, so the $R_{0.1}$ value of SMB is primarily dominated by its entropy elasticity. On the contrary, the temperature sensitivity coefficient ($|K|$) of $R_{3.2}$ from SMB to T4P-SMB decreases gradually, which is attributed to the increase in stiffness elasticity from aged asphalt in the binder. The content of macromolecular heavy components in asphalt increases largely after deep aging, which leads to an increase in the kinetic energy barrier of asphalt molecules; thus, the sensitivity to temperature decreases within a certain range.
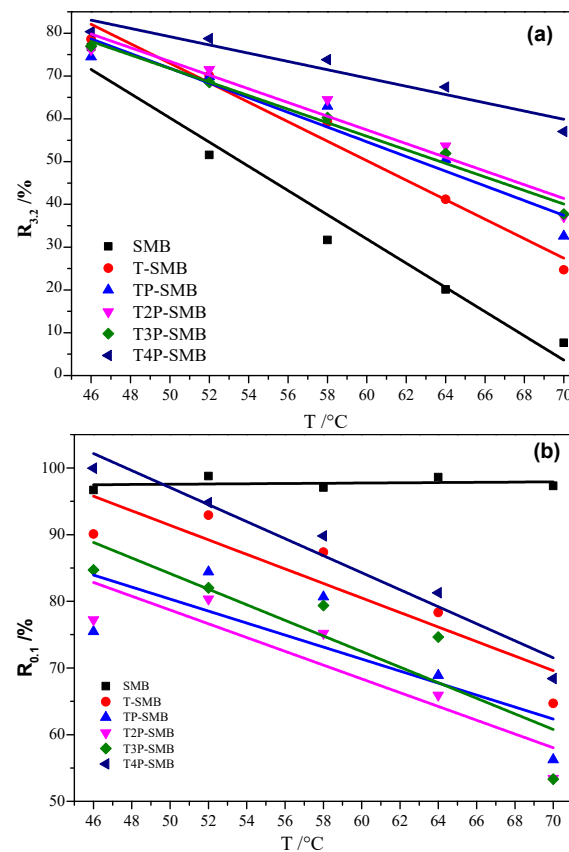
Figure 17. Percentage recovery temperature sensitivity curves of different aged SMBs (**a**): percentage recovery temperature sensitivity under 3.2 kPa; (**b**): percentage recovery temperature sensitivity under 0.1 kPa.

Table 6. Percentage recovery temperature sensitivity equation of all binders.

	$R_{3.2} = KT + B$	$|K|$	$R_{0.1} = KT + B$	$|K|$
SMB	$R_{3.2} = -2.829T + 201.71$	2.829	$R_{0.1} = 0.017T + 96.66$	0.017
T-SMB	$R_{3.2} = -2.278T + 186.89$	2.278	$R_{0.1} = -1.089T + 145.87$	1.089
TP-SMB	$R_{3.2} = -1.718T + 157.73$	1.718	$R_{0.1} = -0.899T + 125.32$	0.899
T2P-SMB	$R_{3.2} = -1.601T + 153.47$	1.601	$R_{0.1} = -1.033T + 130.36$	1.033
T3P-SMB	$R_{3.2} = -1.584T + 150.97$	1.584	$R_{0.1} = -1.168T + 142.61$	1.168
T4P-SMB	$R_{3.2} = -0.965T + 127.48$	0.965	$R_{0.1} = -1.276T + 160.88$	1.276

3.2.6. Fluorescence Micrograph

Fluorescence micrographs of all binders are displayed in Figure 18. Each fluorescence point in a fluorescence micrograph represents the existence of SBS molecules. From Figure 18a, the fluorescent spots are densely distributed and interwoven in the micrograph, which indicates that SBS is uniformly dispersed in SMB and forms a cross-linked network structure. The fluorescent spots are also uniformly and densely distributed in the micrographs of T-SMB from Figure 18b, which suggests that the influence of the mixing and construction processes on the phase state of SBS in SMB is limited. From Figure 18c–f, the fluorescent spots in fluorescence micrographs gradually become sparse until they disappear completely. It implies that the cross-linked structure of SBS in SMB is destroyed, and SBS is gradually oxidized and degraded in service. Simultaneously, the entropy elastic property of SMB gradually weakened to disappear in service, confirming the characteristics of aging matrix asphalt in the above analysis.
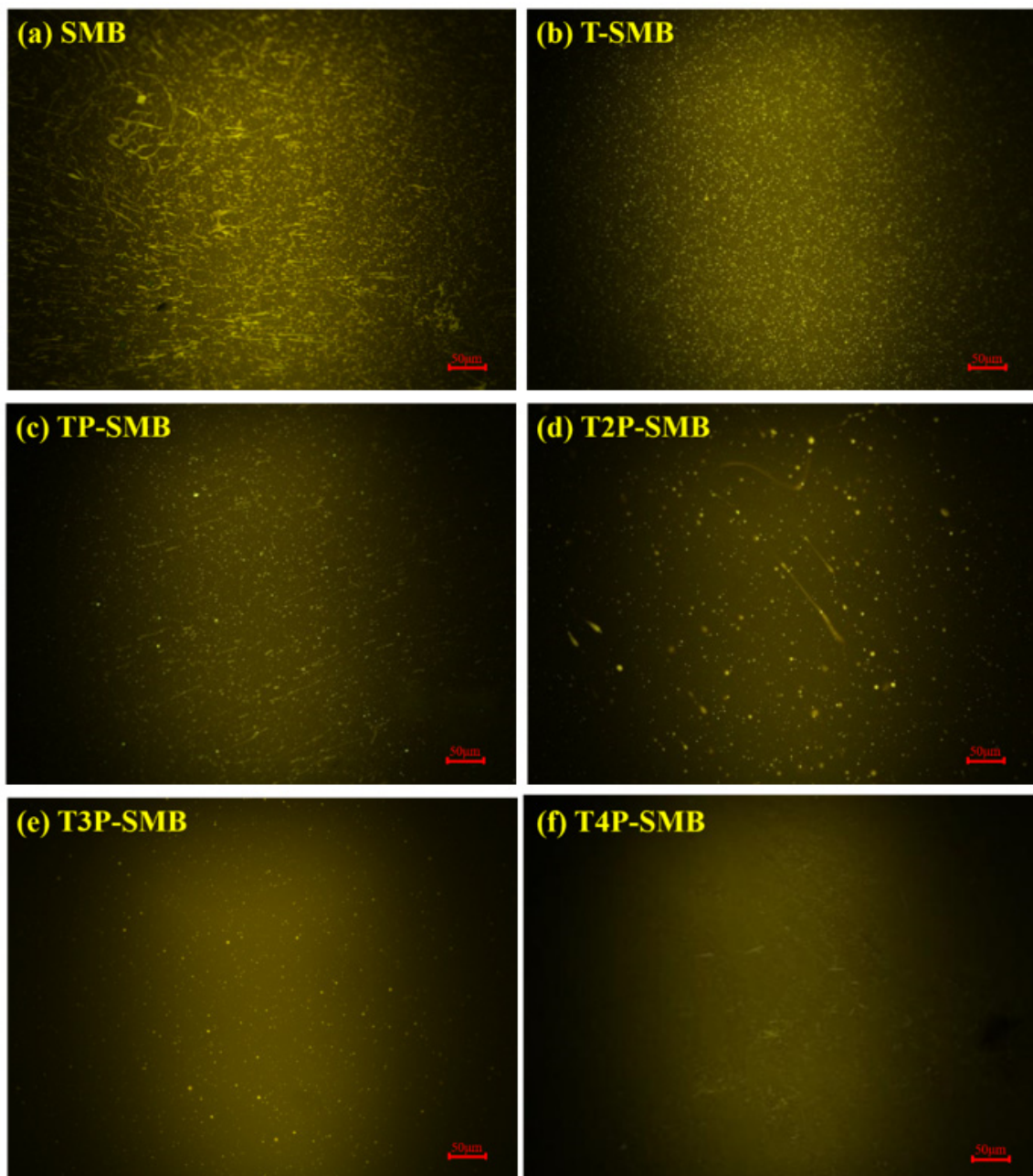
Figure 18. Fluorescence micrograph of all binders.

4. Conclusions

The evolution of the chemical structure, molecular weight and properties of SBS and SMB during the aging process were investigated. Some valuable conclusions are made as follows:

[1] Severe oxygen absorption reactions occur in the aging process of SBS, the polybuta-diene segments in SBS are more susceptible to oxidative degradation as compared with polystyrene segments, and their molecular weight decreases rapidly at the early aging stage;

[2] $I_{C=O}$ and $I_{S=O}$ of SMB increase gradually with the deepening of aging; the structure index of the PB segment in SBS and its molecular weight decrease. The change rate of aging indexes and molecular weight for SMB during the aging process is far less than that of SBS in direct aging, which indicates the aging resistance of the SBS modifier inside asphalt is better than that of the SBS modifier;

[3] The effect of aging on the creep recovery behavior of SMB under high and low shear stresses is quite different; it is due to the combined effect of SBS oxidation degradation and asphalt oxidation hardening;

[4] SBS modifier endows the asphalt with entropy elasticity and reduces its temperature sensitivity. SBS undergoes oxidative degradation as aging progresses, resulting in a gradual weakening of entropy elasticity and an increase in stiffness elasticity;

[5] FM analysis shows the distribution of SBS in SMB gradually becomes sparse and uneven and gradually disappears as aging progresses. It implies that SBS has been completely oxidized and degraded, and the viscoelastic properties of SMB have gradually transformed to those of aged matrix asphalt.

Author Contributions: Investigation, Z.C., Q.H. and K.Q.; methodology, Z.C. and R.Z.; formal analysis, Z.C. and Q.L.; project administration, Z.C.; writing—original draft preparation, Z.C. and Q.H.; writing—review and editing, Z.C. and K.Q.; supervision, X.Q.; funding acquisition, Z.C. and X.Q. All authors have read and agreed to the published version of the manuscript.

Data Availability Statement: Data are contained within the article.

Conflicts of Interest: The authors declare no conflicts of interest.

References

1. Alsolieman, H.A.; Babalghaith, A.M.; Memon, Z.A.; Al-Suhaibani, A.S.; Milad, A. Evaluation and comparison of mechanical properties of polymer-modified asphalt mixtures. *Polymers* **2021**, *13*, 2282. [CrossRef] [PubMed]
2. Chen, Q.; Wang, C.H.; Song, L. Prediction of low-temperature rheological properties of SBS modified asphalt. *Adv. Civ. Eng.* **2020**, *2020*, 8864766. [CrossRef]
3. Milad, A.; Ahmeda, A.G.F.; Taib, A.M.; Rahmad, S.; Solla, M.; Yusoff, N.I.M. A review of the feasibility of using crumb rubber derived from end-of-life tire as asphalt binder modifier. *J. Rubber Res.* **2020**, *23*, 203–216. [CrossRef]
4. Yan, K.; Tian, S.; Chen, J.; Liu, J. High temperature rheological properties of APAO and EVA compound modified asphalt. *Constr. Build. Mater.* **2020**, *233*, 117246. [CrossRef]
5. Cheng, Y.L.; Han, H.Z.; Fang, C.Q.; Li, H.; Huang, Z.; Su, J. Preparation and properties of nano CaCO₃/waste polyethylene/styrene-butadiene-styrene block polymer-modified asphalt. *Polym. Composite* **2019**, *41*, 614–623. [CrossRef]
6. Fang, C.Q.; Qiao, X.T.; Yu, R.E. Influence of modification process parameters on the properties of crumb rubber/EVA modified asphalt. *J. Appl. Polym. Sci.* **2016**, *133*, 43598. [CrossRef]
7. Cuciniello, G.; Leandri, P.; Filippi, S.; Presti, D.L.; Losa, M.; Airey, G. Effect of ageing on the morphology and creep and recovery of polymer-modified bitumens. *Mater. Struct.* **2018**, *51*, 136. [CrossRef]
8. Saboo, N.; Kumar, R.; Kumar, P.; Gupta, A. Ranking the rheological response of SBS- and EVA-Modified Bitumen Using MSCR and LAS Tests. *J. Mater. Civil. Eng.* **2018**, *30*, 04018165. [CrossRef]
9. Mashaan, N.S.; Chegenizadeh, A.; Nikraz, H.; Rezagholilou, A. Investigating the engineering properties of asphalt binder modified with waste plastic polymer. *Ain Shams Eng. J.* **2021**, *12*, 1569–1574. [CrossRef]
10. Behnood, A.; Olek, J. Rheological properties of asphalt binders modified with styrene-butadiene-styrene (SBS), ground tire rubber (GTR), or polyphosphoric acid (PPA). *Constr. Build. Mater.* **2017**, *151*, 464–478. [CrossRef]
11. Song, R.; Sha, A.; Shi, K.; Li, J.; Li, X.; Zhang, F. Polyphosphoric acid and plasticizer modified asphalt: Rheological properties and modification mechanism. *Constr. Build. Mater.* **2021**, *309*, 125158. [CrossRef]
12. Ma, F.; Chen, L.; Zhen, F.; Huang, Y.; Dai, J.; Feng, Q. Evaluation of high temperature rheological performance of polyphosphoric acid-SBS and polyphosphoric acid-crumb rubber modified asphalt. *Constr. Build. Mater.* **2021**, *306*, 124926. [CrossRef]
13. Wang, H.P.; Liu, X.Y.; Zhang, H.; Apostolidis, P.; Erkens, S.; Skarpas, A. Micromechanical modelling of complex shear modulus of crumb rubber modified bitumen. *Mater. Des.* **2020**, *188*, 108467. [CrossRef]
14. Duan, H.; Zhu, C.; Zhang, H.; Zhang, S.; Xiao, F.; Amirkhanian, S. Investigation on rheological characteristics of low-emissions crumb rubber modified asphalt. *Int. J. Pavement Eng.* **2023**, *24*, 2164891. [CrossRef]
15. Zhang, W.; Ma, T.; Xu, G.; Huang, X.; Ling, M.; Chen, X.; Xue, J. Fatigue resistance evaluation of modified asphalt using a multiple stress creep and recovery (MSCR) test. *Appl. Sci.* **2018**, *8*, 417. [CrossRef]
16. Xiong, J.; Xuan, W.; Feng, M.; Ma, F. The performance of SBS modified asphalt binder base on the MSCR test. *IOP Conf. Ser. Mater. Sci. Eng.* **2019**, *631*, 022018. [CrossRef]

17. Babagoli, R.; Vamegh, M.; Mirzababaei, P. Laboratory evaluation of the effect of SBS and Lucobite on performance properties of bitumen. *Petrol. Sci. Technol.* **2018**, *30*, 255–260. [CrossRef]
18. Joohari, I.B.; Giustozzi, F. Oscillatory shear rheometry of hybrid polymer-modified bitumen using multiple stress creep and recovery and linear amplitude sweep tests. *Constr. Build. Mater.* **2022**, *315*, 125791. [CrossRef]
19. Luo, X.; Ling, J.; Li, H.; Zhang, Y.; Li, Y. Nonlinear viscoelastoplastic kinetics for high-temperature performance of modified asphalt binders. *Mech. Mater.* **2023**, *180*, 104612. [CrossRef]
20. Yang, Z.; Zhang, X.; Yu, J.; Xu, W. Effects of aging on the multiscale properties of SBS-modified asphalt. *Arab. J. Sci. Eng.* **2019**, *44*, 4349–4358. [CrossRef]
21. Xu, G.; Yao, Y.; Wu, M.; Zhao, Y. Molecular simulation and experimental analysis on co-aging behaviors of SBS modifier and asphalt in SBS-modified asphalt. *Mol. Simulat.* **2023**, *49*, 629–642. [CrossRef]
22. Yu, H.; Bai, X.; Qian, G.; Wei, H.; Gong, X.; Jin, J.; Li, Z. Impact of ultraviolet radiation on the aging properties of SBS-modified asphalt binders. *Polymers* **2019**, *11*, 1111. [CrossRef] [PubMed]
23. Chen, H.; Qiu, H.; Wu, Y.; Kuang, D.; Xing, M. Aging resistance of SBS-SBR composite modified asphalt materials for high altitude and cold regions. *Mater. Struct.* **2022**, *55*, 187. [CrossRef]
24. Eltwati, A.; Al-Saffar, Z.; Mohamed, A.; Hainin, M.R.; Elnihum, A.; Enieb, M. Synergistic effect of SBS copolymers and aromatic oil on the characteristics of asphalt binders and mixtures containing reclaimed asphalt pavement. *Constr. Build. Mater.* **2022**, *327*, 127026. [CrossRef]
25. Wang, F.; Zhang, L.; Zhang, X.; Li, H.; Wu, S. Aging mechanism and rejuvenating possibility of SBS copolymers in asphalt binders. *Polymers* **2020**, *12*, 92. [CrossRef]
26. *ASTM Standard D36*; Standard Test Method for Softening Point of Bitumen (Ring-and-Ball Apparatus). American Society for Testing and Materials: West Conshohocken, PA, USA, 2006.
27. *ASTM Standard D113*; Standard Test Method for Ductility of Asphalt Materials. American Society for Testing and Materials: West Conshohocken, PA, USA, 2007.
28. *ASTM Standard D5*; Standard Test Method for Penetration of Bituminous Materials. American Society for Testing and Materials: West Conshohocken, PA, USA, 2013.
29. *ASTM Standard D4402*; Standard Test Method for Viscosity Determination of Asphalt at Elevated Temperatures Using a Rotational Viscometer. American Society for Testing and Materials: West Conshohocken, PA, USA, 2015.
30. Liu, H.; Zeiada, W.; Al-Khateeb, G.G.; Shanableh, A.; Samarai, M. Use of the multiple stress creep recovery (MSCR) test to characterize the rutting potential of asphalt binders: A literature review. *Constr. Build. Mater.* **2021**, *269*, 121320. [CrossRef]
31. Yan, C.; Huang, W.; Xiao, F.; Wang, L.; Li, Y. Proposing a new infrared index quantifying the aging extent of SBS-modified asphalt. *Road Mater. Pavement.* **2017**, *19*, 1406–1421. [CrossRef]
32. Xu, X.; Yu, J.; Zhang, C.; Xu, S.; Xue, L.; Xie, D. Investigation of aging behavior and thermal stability of styrene-butadiene-styrene tri-block copolymer in blends. *Polymers* **2016**, *40*, 947–953. [CrossRef]
33. Lamontagne, J. Comparison by Fourier transform infrared (FTIR) spectroscopy of different ageing techniques: Application to road bitumens. *Fuel* **2001**, *80*, 483–488. [CrossRef]
34. Cao, Z.L.; Chen, M.Z.; Yu, J.Y.; Han, X.B. Preparation and characterization of active rejuvenated SBS modified bitumen for the sustainable development of high-grade asphalt pavement. *J. Clean Prod.* **2020**, *273*, 123012. [CrossRef]
35. Zhou, T.; Cao, L.; Fini, E.H.; Li, L.; Liu, Z.; Dong, Z. Behaviors of asphalt under certain aging levels and effects of rejuvenation. *Constr. Build. Mater.* **2020**, *249*, 118748. [CrossRef]
36. Cao, Z.L.; Chen, M.Z.; He, B.Y.; Han, X.; Yu, J.; Xue, L. Investigation of ultraviolet aging resistance of bitumen modified by layered double hydroxides with different particle sizes. *Constr. Build. Mater.* **2019**, *196*, 166–174. [CrossRef]
37. Johnson, C.M.; Bahia, H.; Wen, H.F. Practical application of viscoelastic continuum damage theory to asphalt binder fatigue characterization. *Asph. Paving Technol.-Proc.* **2009**, *78*, 597–638.